European Journal of Cardio-Thoracic Surgery 0 (2017) 1–7
doi:10.1093/ejcts/ezx207

ORIGINAL ARTICLE

Cite this article as: Mao Y, Chi C, Yang F, Zhou J, He K, Li H *et al*. The identification of sub-centimetre nodules by near-infrared fluorescence thoracoscopic systems in pulmonary resection surgeries. Eur J Cardiothorac Surg 2017; doi:10.1093/ejcts/ezx207.

THORACIC

The identification of sub-centimetre nodules by near-infrared fluorescence thoracoscopic systems in pulmonary resection surgeries

Yamin Mao[a,b,c,†], Chongwei Chi [a,b,c,†], Fan Yang[d,†], Jian Zhou[d,†], Kunshan He[a,b,c], Hao Li[d], Xiuyuan Chen[d], Jinzuo Ye[a,b,c], Jun Wang[d] and Jie Tian[a,b,c,*]

[a] CAS Key Laboratory of Molecular Imaging, Institute of Automation, Chinese Academy of Sciences, Beijing, China
[b] School of Computer and Control Engineering, University of Chinese Academy of Sciences, Beijing, China
[c] Beijing Key Laboratory of Molecular Imaging, Chinese Academy of Sciences, Beijing, China
[d] Department of Thoracic Surgery, Peking University People's Hospital, Beijing, China

* Corresponding author. CAS Key Laboratory of Molecular Imaging, Institute of Automation, Chinese Academy of Sciences, Beijing 100190, China. Tel: +86-010-82628760; fax: +86-010-62527995; e-mail: jie.tian@ia.ac.cn (J. Tian).

Received 11 February 2017; received in revised form 20 April 2017; accepted 3 May 2017

Abstract

OBJECTIVES: Current surgical procedures lack high-sensitivity intraoperative imaging guidance, leading to undetected micro tumours. *In vivo* near-infrared (NIR) fluorescence imaging provides a powerful tool for identifying small nodules. The aim of this study was to examine our experience of using 2 different NIR devices in pulmonary resection surgery.

METHODS: From August 2015 to October 2016, 36 patients with lung nodules underwent NIR fluorescence imaging thoracoscopic surgery. Two NIR devices: a D-Light P system and a SUPEREYE system were used. Patients were administered an injection of indocyanine green (ICG) through the peripheral vein 24 h preoperatively. During surgery, traditional white-light thoracoscopic exploration was performed first, followed by ICG-fluorescent-guided exploration. All detected nodules were resected and examined by a pathologist.

RESULTS: Of the 36 patients, 76 nodules were resected. ICG-fluorescent imaging identified 68 nodules during *in vivo* exploration. The mean signal-to-background ratio of lung nodules in NIR exploration was 3.29 ± 1.81. The application of NIR devices led to the detection of 9 additional nodules that were missed using traditional detection methods (1 mm computed tomography scan and white-light thoracoscopic exploration) in 7 patients (19.4%). Four of the 9 nodules were confirmed as malignant or atypical adenomatous hyperplasia (44.4%). The other 5 nodules were confirmed as false-positive nodules. The sensitivities and positive predictive values of the ICG-fluorescent imaging for lung tumours were 88.7% and 92.6%, respectively.

CONCLUTIONS: This study demonstrated the feasibility and safety of using ICG-fluorescent imaging for multiple lung nodules identification in video-assisted thoracoscopic surgery pulmonary resection.

Clinicaltrial.gov number: NCT02611245.

Keywords: Lung cancer • Video-assisted thoracoscopic surgery • Cancer imaging • NIR fluorescence imaging • ICG

INTRODUCTION

Lung cancer is the most common cancer type and the leading cause of cancer death in China [1]. Up to 15% of lung cancer patients develop synchronous or metachronous nodules [2, 3]. Meanwhile, when dealing with pulmonary metastasis tumours of other malignancies, the detection of all nodules is also challenging. Failure to remove all of the micro lesions during surgery might be one of the causes of recurrence. With the widespread use of video-assisted thoracoscopic surgery (VATS), manual palpation of pulmonary nodules is restricted; surgeons have to rely on visual inspection. However, white-light imaging as the primary intraoperative imaging method lacks the contrast between tumours and normal tissue [4]. For the current clinical imaging methods, superficially multiple micro lesions with a diameter of <5 mm are particularly difficult to detect [5]. Thus, patients with lung nodules need a new imaging technology to better identify small lung lesions and guide surgery in real time [6].

Fluorescence image-guided surgery is a highly sensitive and specific imaging method that has the potential to identify imperceptible lesions [7–9]. Currently, the most widely used NIR fluorescence dye is indocyanine green (ICG) (excitation: 778 nm and emission: 830 nm), which was approved by the Food and Drug Administration (FDA). The ICG is a very safe imaging agent that has few allergic reactions (approximately 0.003%) and is applied in various tumour detection because of its passive accumulation

†The first four authors contributed equally to this work.

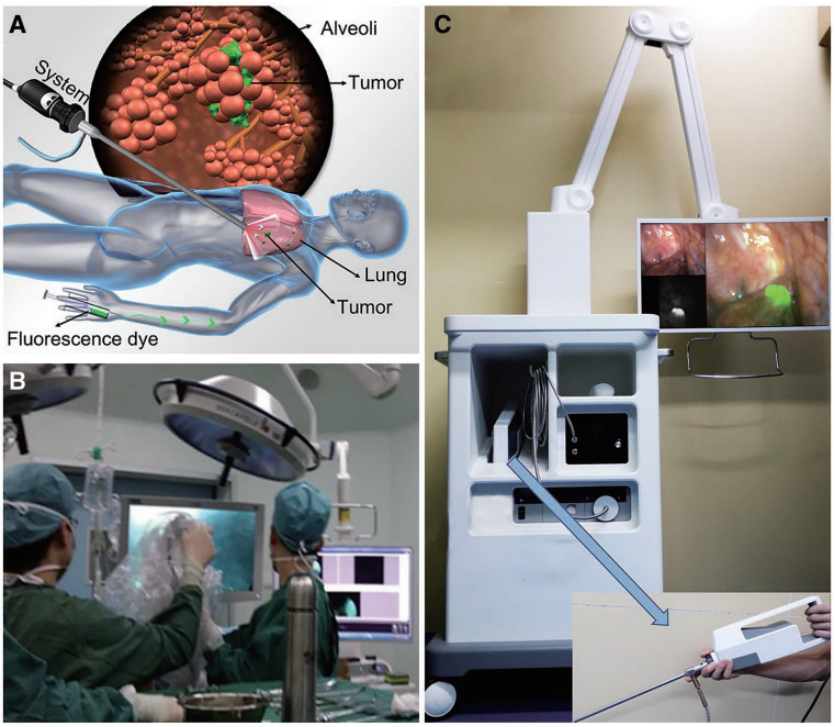

Figure 1: The design and clinical application of the SUPEREYE. (**A**) Schematic illustrations of our fluorescence thoracoscopic system used for lung cancer surgery. Patients were firstly injected with fluorescence dyes for labelling imaging region. NIR excited light and white light simultaneously illuminated the imaging region through the thoracoscope. Then our system provided the optical guidance about the spatial localization of tumours. (**B**) The SUPEREYE was applied in video-assisted thoracoscopic surgery lung cancer surgery. (**C**) The SUPEREYE.

[10]. Several groups have proved the feasibility and benefits of near-infrared (NIR) fluorescence image-guided surgery in tumour nodules detection [11–16]. van Dam *et al.* showed that the use of fluorescence imaging technology detected significantly additional tumour nodules in ovarian cancer surgery [17]. Liberale *et al.* showed that NIR image-guided surgery discovered a higher number of subclinical lesions than conventional inspection for peritoneal carcinomatosis [18]. Moreover, Okusanya *et al.* performed open surgeries of lung cancer and successfully confirmed that ICG could remain in tumours 24 h after intravenous injection by enhanced permeability and retention (EPR) effect. They detected 5 additional non-palpable nodules guided by NIR fluorescence imaging [19]. Compared with open surgery, the treatment of lung cancer with VATS showed an urgent demand for fluorescence imaging guidance due to less manual palpation and more undiscovered additional nodules [20, 21]. However, research in this field has been restricted due to the lack of high-sensitivity fluorescence thoracoscopic systems. To satisfy this need, we developed a novel ultrasensitive fluorescence thoracoscopic system (SUPEREYE) that offers high-fluorescence collection efficiency and accurate registration. High sensitivity of imaging systems collects weak signals of small tumours. Furthermore, easy, robust and quick image registration can provide real-time white-light and fluorescence imaging guidance in lung cancer surgery.

The purpose of this study was to analyse our experience with 2 different NIR devices: the SUPEREYE system by Key Laboratory of Molecular Imaging, Chinese Academy of Science and the D-Light P system by Karl Storz Company, in pulmonary resection surgeries. We found that ICG-fluorescent imaging has the potential to detect small subclinical lung nodules. In this pilot study, we recruited 36 patients and reported the results of tumour imaging in NIR fluorescence image-guided lung cancer thoracoscopic surgery.

MATERIALS AND METHODS

Fluorescence thoracoscopic system

The SUPEREYE is a fluorescence thoracoscopic system developed for image-guided minimally invasive surgery. This system contains a colour imaging channel (400–650 nm) and a NIR fluorescence imaging channel (excitation: 785 ± 5 nm; emission: 840 ± 10 nm). Fluorescence imaging was designed especially for collecting the wavelength of ICG. We designed the system based on 3 aspects: (i) Image acquisition: a NIR light-optimum rigid clinical thoracoscope (HOPKINS II 26003BGA, Karl Storz, Tuttlingen, Germany) was used as system lens. The light collected from the lens is transmitted into a customized camera (Microview, Beijing, China). The camera contains 1 light splitter and 2 high-sensitivity and high-resolution camera chips for simultaneous colour and NIR fluorescence imaging. (ii) Illumination design: one 785-nm NIR excitation light source (MW-SGX-785, Changchun Lei Shi Optoelectronic Technology Co. Ltd, Changchun, Jilin, China) and one visible light source (XENON NOVA 300, Karl Storz) were coupled by a custom-made multimode bifurcated fibre bundle (Banglei Optoelectronic Technology Co. Ltd, Zhongshan, Guangdong, China) with small light coupling loss. (iii) Software development: the collected fluorescence and colour images can be accurately, quickly and robustly registered into merged images. The software simultaneously displays colour, fluorescence and merged images at a video rate. The spatial resolution of the system is 35 μm, and the sensitivity for ICG detection is 0.01 μm. We also used another commercial fluorescence thoracoscopic system to explore the feasibility of lung tumours detection: the D-Light P system (Karl Storz). This system sensitivity is 0.1 μm but

currently it cannot simultaneously display colour and fluorescence images.

Patients

This study enrolled 36 patients (19 males and 17 females) who were scheduled for VATS pulmonary resection surgery in Peking University People's Hospital. The hospital's Institutional Review Board approved this study (2015PHB157-01), and all patients signed the informed consents. We also registered this clinical trial at ClinicalTrials.gov (NCT02611245). All patients had one or more pulmonary nodules diagnosed by chest high-resolution computed tomography (CT) with 0.1 cm slice thickness. Patients who had ICG allergy were excluded.

Imaging procedure

Intraoperative lung cancer thoracoscopic surgery was guided by traditional white-light imaging and ICG-fluorescent imaging. Figure 1 illustrates the NIR fluorescence imaging-guided lung cancer surgery. Patients were administered ICG (Yichuang Pharmaceutical Limited Liability Company, Dandong, China) at a dose of 5 mg/kg according to patients' weight through a peripheral vein 24 h preoperatively [22]. The fluorescence thoracoscopic system was prepared and covered with a sterilized set. In the first step, surgeons located tumours according to a traditional standard operating procedure, which combined preoperative CT data and white-light thoracoscopy. In the next step, the detected lung nodules were subsequently investigated by the fluorescence thoracoscopic system. The colour, fluorescence and merged images of the nodules were simultaneously displayed and recorded at video rate. Meanwhile, we grossly examined the lung for extra subclinical tumour nodules detection in this procedure. All identified nodules were removed and marked for biopsies. The specimens were reviewed by 2 experienced pathologists (Kunkun Sun and Danhua Shen).

Analysis of fluorescence data

Fluorescence intensity of lung lesions was quantitatively analysed according to the recorded videos. The calculation method was as follows: we used an image processing software (ImageJ, National Institutes of Health, Bethesda, MD, USA) to delineate lung nodule as a region of interest (ROI), and then the software calculated the mean brightness value of ROI (B_{ROI}) within a range of 0–255. The background brightness ($B_{Background}$) was measured by calculating the mean brightness value of surrounding tissues. The signal-to-background ratio (SBR) was calculated by dividing the B_{ROI} by the $B_{Background}$. Each nodule was evaluated 3 times to reduce errors.

Statistical analysis

To compare the fluorescence intensity differences obtained while using the 2 fluorescence imaging systems (SUPEREYE and D-Light P), we performed Student's *t*-tests. The analysis was performed using Prism software version 4.0 (San Diego, CA, USA). Two-sample, one-way Student's *t*-tests were used to determine significant differences in the hypothesis that the SBR of SUPEREYE was higher than the SBR of D-Light P. If the *P*-value was <0.05, the SBR differences were considered to be valid.

Table 1: Individual data for patients ($n = 36$)

Characteristics	Value
Age (year)	56 ± 14
Gender (patients)	Men = 19; Woman = 17
Tumour size (cm)	1.4 ± 1.2
SBR [range]	
Tumour size >1cm	3.46 (1.43–11.90)
Tumour size ≤1cm	3.14 (1.47–7.67)
Tumour location (nodules)	
RUL	16
RML	12
RLL	28
LUL	11
LLL	9
Pathology (nodules)	SBR [range]
Adenocarcinoma (30)	2.91 (1.43–7.13)
SCC (4)	4.08 (2.75–5.12)
Breast (2)	3.29 (3.21–3.38)
HCC (11)	6.09 (3.97–11.9)
Colorectal cancer (11)	3.03 (1.87–5.16)
Osteosarcoma (10)	2.13 (1.90–2.52)
AAH (2)	2.66 (2.47–2.85)
Hyperplasia (5)	1.98 (1.53–3.6)
Inflammation (1)	3.57
System (nodules)	SBR [range]
SUPEREYE (19)	3.83 (2.25–7.13)
D-Light P (57)	3.11 (1.43–11.9)

SBR: signal-to-background ratio; RUL: right upper lobe; RML: right middle lobe; RLL: right lower lobe; LUL: left upper lobe; LLL: left lower lobe; SCC: squamous cell carcinoma; HCC: hepatocellular carcinoma; AIS: adenocarcinoma *in situ*; AAH: atypical adenomatous hyperplasia.

RESULTS

Characteristics of lung nodules

From August 2015 to October 2016, we enrolled 36 patients (age 56 ± 14 years) in this study. In total, 76 nodules (size 1.4 ± 1.2 cm) were detected by combining traditional methods with ICG-fluorescent imaging. From the 36 patients, 11 patients were diagnosed with metastasis from other cancers and 25 patients with non-small-cell lung cancer (NSCLC) (Table 1). We performed wedge resection in 14 patients, segmentectomy in 7 patients, lobectomy in 14 patients and pneumonectomy in 1 patient.

The ICG-fluorescent imaging method successfully identified 68 of the 76 nodules *in vivo*. The other 8 nodules that were located 1.3 cm or more beneath the pleural surface could not be detected. After excision and direct exposure of these nodules, all 76 nodules were fluorescent. Histology of these nodules showed that 71 pulmonary nodules were malignant and 5 nodules were false positive (hyperplasia and inflammation). The characteristics of the nodules are listed in Table 1. The mean SBR of the nodules was 3.29 ± 1.81 (range: 1.43–11.9). The 2 NIR devices could high-sensitivity detect lung nodules in pulmonary resection surgery (Fig. 2). We found that ICG-fluorescent imaging had a great imaging effect for squamous cell carcinoma (SBR: 4.08 ± 0.88) and pulmonary metastasis of hepatocellular carcinoma (HCC) (SBR: 6.09 ± 2.4). The mean SBR of adenocarcinoma nodules was 2.91. However, in some adenocarcinoma nodules, the SBR was as low as 1.43 and the contrast between the nodules and the surrounding tissues was less obvious.

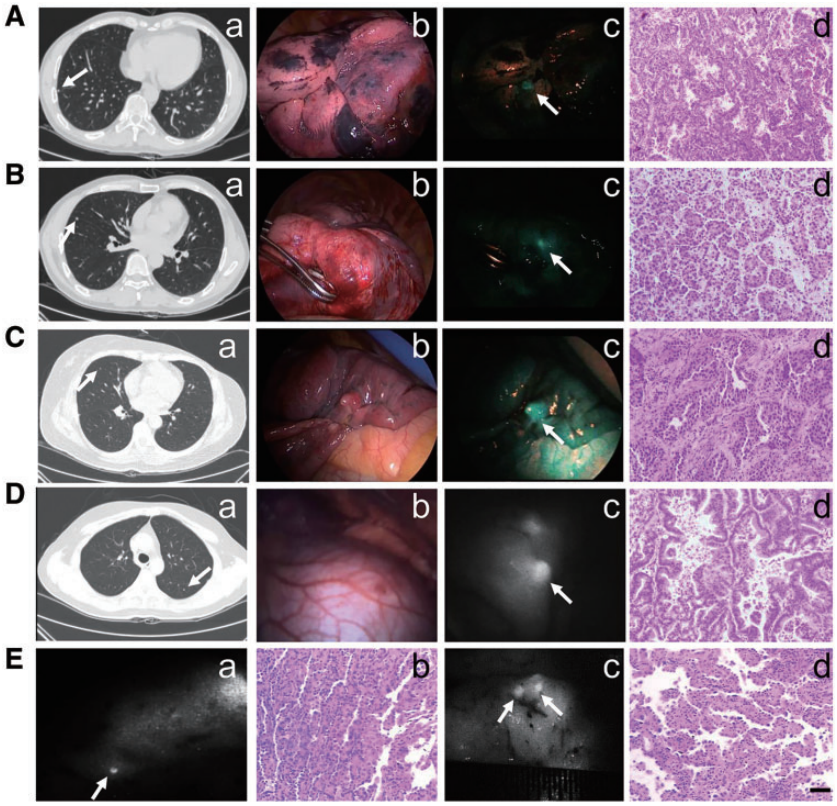

Figure 2: *In vivo* sub-centimetre pulmonary tumours imaging with near-infrared fluorescence thoracoscopic systems. (a–d) of (**A–D**): Computed tomography, colour, fluorescence and haematoxylin and eosin staining images of pulmonary tumours (white arrow). (**A**) Adenocarcinoma, tumour size: 0.5 cm; (**B**) pulmonary metastases of hepatocellular carcinoma, tumour size: 0.5 cm; (**C**) pulmonary metastases of breast cancer, tumour size: 1 cm; (**D**) pulmonary metastases of colorectal cancer, tumour size: 1 cm. (**E**) Additional pulmonary nodules only detected by indocyanine green-fluorescent imaging; (a) and (c) are representative fluorescence images of additional nodules (white arrow) (tumour size: 0.1 cm, 0.2 cm, 0.2 cm); (b) and (d) are the corresponding haematoxylin and eosin staining images showing that (a) is atypical adenomatous hyperplasia and (c) is adenocarcinoma *in situ*. Scale bar: 50 μm.

The sensitivities and positive predictive values of ICG-fluorescent imaging for lung tumours were thus 88.7% (63 fluorescing lesions of the 71 malignant nodules) and 92.6% (63 cancers of the 68 fluorescing lesions), respectively.

Indocyanine green-fluorescent imaging can identify sub-centimetre lung nodules

Although preoperative imaging provided information on the location of small nodules, it remains a challenge to localize sub-centimetre pulmonary nodules by VATS. To examine our experience of using ICG-fluorescent imaging to detect micro nodules, 2 NIR devices were used during surgery. For lung nodules with a size ≤1 cm, the fluorescence signals were clearly demarcated from the surrounding normal tissues with a mean SBR of 3.14 ± 1.59. ICG-fluorescent images collected either by our self-developed system (SBR: 3.83 ± 1.24) or by a commercial fluorescence thoracoscopic system (SBR: 3.11 ± 1.94) showed a significant tumour-to-surrounding tissue contrast compared with the traditional white-light imaging (Fig. 3).

Figure 2A–D shows the CT, colour, fluorescence and haematoxylin and eosin (H&E) of micro pulmonary nodules (adenocarcinoma, pulmonary metastases of HCC, breast cancer and colorectal cancer). Notably, all of these tumours were less than 1 cm.

Indocyanine green-fluorescent imaging can identify additional pulmonary nodules

Among the 76 nodules, 9 additional small lung nodules were detected only by the ICG-fluorescent imaging method in 7 of the 36 patients (19.4%). For the 9 nodules, 6 nodules were detected in different lobes than the primary tumours. The characteristics of these nodules are shown in Table 2. These 9 lesions comprised 2 adenocarcinoma *in situ*, 2 atypical adenomatous hyperplasia, and 5 false-positive nodules (hyperplasia and inflammation). The representative frames of additional small nodules and the corresponding histopathological results are shown in Fig. 2E (white arrow). They were missed by traditional white-light thoracoscopic exploration and CT images. In contrast, ICG-fluorescent imaging showed the 3 additional synchronous nodules with high SBR (2.85 ± 0.11, 2.47 ± 0.14 and 2.25 ± 0.18). The tumour size were ≤0.2 cm. Histology results of these nodules were atypical adenomatous hyperplasia and adenocarcinoma *in situ* (Fig. 2E).

DISCUSSION

In the treatment of malignant lung nodules, the efficacy of surgical resection remains limited by the lack of real-time high-sensitivity intraoperative imaging methods. Furthermore, incomplete resection results in postoperative recurrence of the

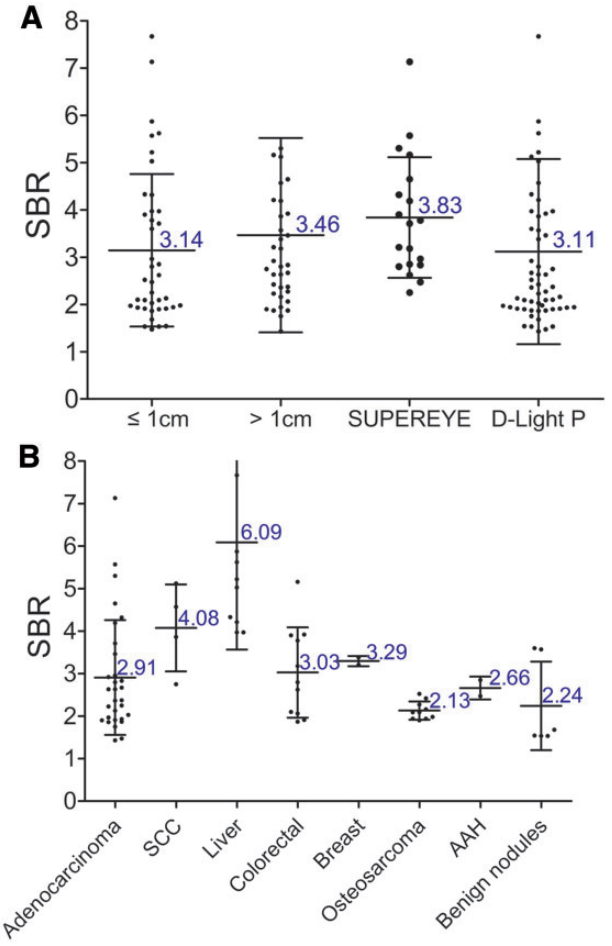

Figure 3: Fluorescence data of pulmonary nodules. (**A**) The SBR of tumour size ≤1 cm and >1 cm, and SBR of fluorescence images collected by our system (SUPEREYE) and by the commercial system (D-Light P). (**B**) SBR of different pulmonary nodules types. SBR: signal-to-background ratio.

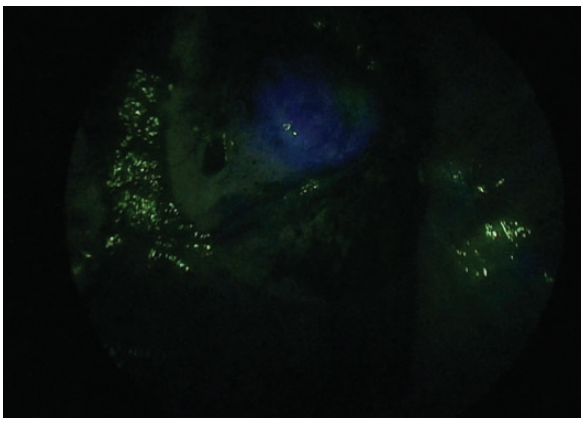

Video 1: The video of pulmonary nodules with 2 NIR devices. The video displays real-time intraoperative fluorescence imaging of pulmonary adenocarcinoma, squamous cell carcinoma, metastasis of osteosarcoma, metastasis of colorectal cancer, metastasis of hepatocellular carcinoma, metastasis of breast cancer, and additional detected nodules.

malignancy. Therefore, the development of new high-sensitivity imaging methods, such as ICG-fluorescent imaging, shows great potential to detect additional subclinical nodules.

ICG is not a tumour-specific fluorescence dye, such as ligand-specific binding to tumour cell receptor, it accumulates in certain types of tumours because of the EPR effect [23–25]. The EPR effect is a passively accumulating effect due to the permeability effect of the nascent porous tumour blood vessels and the retention effect of dysfunctional tumour lymphatic system, which allows ICG to accumulate in tumour tissues. To obtain an optimal tumour-to-lung contrast, we have performed several pre-experiments of injection dose and time of ICG. The results demonstrated that the optimum dose was 5 mg/kg and that the best injection time was 24 h preoperatively. In combination with ICG, fluorescence imaging provided high-contrast tumour images and increased additional tumour detection rate. Okusanya *et al.* first demonstrated ICG could be applied for lung nodules imaging and verified ICG-fluorescent imaging guided open surgery could detect additional pulmonary nodules. However, in the treatment of lung cancer by VATS, only a few research studies have explored the application of ICG-fluorescent imaging [26], but the sensitivity and specificity of ICG-fluorescent image-guided lung cancer thoracoscopic surgery have not been studied.

Table 2: Characteristics of the nodules identified only by ICG-fluorescent imaging

Patient no.	Cancer location	SBR	Histopathology	Tumour size (cm)
3	LUL	2.25 ± 0.18	AIS	0.1
6	RLL	2.85 ± 0.11	AAH	0.2
6	RLL	2.47 ± 0.14	AAH	0.2
13	RUL	1.68 ± 0.03	Hyperplasia	0.3
13	RLL	1.53 ± 0.05	Hyperplasia	0.2
18	RLL	1.96 ± 0.08	AIS	0.1
25	LLL	3.57 ± 0.13	Inflammation	1.5
32	RLL	3.60 ± 0.03	Hyperplasia	0.3
34	RUL	1.53 ± 0.09	Hyperplasia	0.5

AIS: adenocarcinoma in situ; AAH: atypical adenomatous hyperplasia; ICG: indocyanine green.

More early stage lung cancer patients chose VATS as a superior alternative to open surgery due to minimal trauma, less bleeding and faster recovery, while the fluorescence thoracoscopic system applied in VATS was faced with a big challenge [27]. The poor NIR-light transmission and small apertures of the traditional white-light thoracoscope resulted in a massive light loss and low tumour-to-tissue contrast. Thus, many researchers have devoted themselves to developing high-sensitivity NIR fluorescence thoracoscopic systems. Venugopal *et al.* simultaneously optimized NIR fluorescence and colour imaging using a custom endoscope and a 2-charge-coupled device (CCD) camera [28]. Glatz *et al.* used a more sensitive electron-multiplying charge-coupled device camera to improve the NIR wavelength collection efficiencies [29]. In our case, we designed a fluorescence thoracoscopic system specially for ICG imaging. Its sensitivity for ICG imaging is about 10 times higher than that of the published fluorescence thoracoscopic system [28]. And we also used a commercial fluorescence imaging system (D-Light P) in this study.

The goal of our study was to validate our experience of using 2 different NIR devices, enabling high-sensitivity identification of sub-centimetre pulmonary nodules in VATS lung cancer surgery. For sub-centimetre lung nodules, the commercial D-Light P system showed a significant tumour-to-surrounding tissue contrast (SBR: 2.91 ± 1.62) compared with traditional white-light imaging. We found that ICG-fluorescent imaging had a higher SBR in

squamous cell carcinoma and pulmonary metastasis of HCC than other lung tumours. The possible reason is that squamous cell carcinoma is an epithelial tumour that has both an exceptionally high endocytic rate and deficient tight junctions that lead to more ICG accumulating in cells. Furthermore, the HCC tumour cells expressed the membrane transporters' organic anion transporting polypeptide 1B3 and sodium–taurocholate co-transporting polypeptide, which mediates the cellular uptake of ICG [30]. A more detailed study would need to be performed to validate the relation between SBR and histopathology. Furthermore, our self-developed SUPEREYE system has a higher SBR of 3.69 ± 1.37 than D-Light P ($P < 0.05$). For the detected 76 nodules, the sensitivities and positive predictive values of the ICG-fluorescent imaging were 88.7% and 92.6%. Eight pulmonary nodules embedded deeply in the lung were undetected by ICG-fluorescent imaging, and the maximized detection depth of ICG-fluorescent method was 1.3 cm. Future studies on fluorescence thoracoscopic systems should focus on developing deep tissue imaging with new imaging technologies, such as a second NIR imaging method (wavelength: 1100–1400 nm).

Furthermore, we detected 4 additional positive nodules that were not revealed during standard surgical exploration. If these extra subclinical nodules were not resected, recurrence or metastasis of lung tumours might result in poor prognosis. Meanwhile, the extra resections were safe without obvious/prolong air leak. However, we also detected 5 additional false-positive nodules with the ICG-fluorescent imaging method. The histopathology results of these false-positive nodules were hyperplasia or inflammation. ICG as a non-specific fluorescence dye was diffused into tissues with hyperpermeable vascular structures by EPR effect, such as hyperplasia or inflammation. To reduce the false-positive results, surgeons could use alternative indications (inspection and palpation of nodules) to judge whether the fluorescence area should be removed or not. Targeted NIR probes that specifically bind lung tumour tissues have the potential to decrease false-positive nodules. Therefore, further studies will need to develop novel NIR targeting agents for increasing positive predictive values.

Currently, it is difficult to distinguish small multiple nodules from surrounding tissues via intraoperative white-light thoracoscopy, however, the ICG-fluorescent imaging method is good for sub-centimetre tumour detection. Therefore, by combining ICG-fluorescent imaging with preoperative CT data, the surgical exploration in pulmonary resections reveals the nodules located deeply in the lung and easily identifies sub-centimetre nodules. As a result, exploration time might be saved and the tumour detection rate might be improved. The next obvious step for us is to design a random, double-blind and multiple study to compare ICG-fluorescent imaging combining CT method with the traditional white-light imaging combining CT method for the detection of pulmonary nodules.

CONCLUSION

In conclusion, we believe we have validated that ICG-fluorescent imaging with 2 NIR devices enables high-sensitivity visualization of sub-centimetre pulmonary nodules. In addition, we showed that ICG-fluorescent imaging also has the potential to detect additional positive lesions. The identification of these nodules might reduce tumour recurrence, which has a remarkable clinical potential for application in lung cancer.

ACKNOWLEDGEMENTS

We thank Lixue Zhang for his help with the clinical experiments, Kunkun Sun and Danhua Shen for the pathological analysis and Yu An and Shixin Jiang for the helpful discussions.

Funding

This work was supported by the National Natural Science Foundation of China [81227901, 81527805, 81501594, 61231004, 61501462, 61671449], the National Key Research Program [2017YFA0205200], the National Key Project of the Ministry of Science and Technology of China [2106YFC0103702], the Scientific Research and Equipment Development Project of Chinese Academy of Sciences [YZ201457] and the Key Research Program of the Chinese Academy of Sciences [KGZD-EW-T03].

Conflict of interest: none declared.

REFERENCES

[1] Chen W, Zheng R, Baade PD, Zhang S, Zeng H, Bray F *et al*. Cancer statistics in China, 2015. CA Cancer J Clin 2016;66:115.
[2] Aliperti LA, Predina JD, Vachani A, Singhal S. Local and systemic recurrence is the Achilles heel of cancer surgery. Ann Surg Oncol 2010;18:603–7.
[3] van Rens MT, Schramel FM, Elbers JR, Lammers JW. The clinical value of lung imaging fluorescence endoscopy for detecting synchronous lung cancer. Lung Cancer 2001;32:13–8.
[4] Glatz J, Garcia-Allende PB, Becker V, Koch M, Meining A, Ntziachristos V. Near-infrared fluorescence cholangiopancreatoscopy: initial clinical feasibility results. Gastrointest Endosc 2014;79:664–8.
[5] Keating JJ, Kennedy GT, Singhal S. Identification of a subcentimeter pulmonary adenocarcinoma using intraoperative near-infrared imaging during video-assisted thoracoscopic surgery. J Thorac Cardiovasc Surg 2015;149:e51–3.
[6] Liu B, Feng Y, Zhang J, Li H, Li X, Jia H *et al*. Imaging of bronchioloalveolar carcinoma in the mice with the $\alpha_v\beta_3$integrin-targeted tracer 99m Tc-RGD-4CK. Transl Res 2013;162:174–80.
[7] Chi C, Du Y, Ye J, Kou D, Qiu J, Wang J *et al*. intraoperative imaging-guided cancer surgery: from current fluorescence molecular imaging methods to future multi-modality imaging technology. Theranostics 2014;4:1072–84.
[8] Vahrmeijer AL, Hutteman M, van der Vorst JR, van de Velde CJ, Frangioni JV. Image-guided cancer surgery using near-infrared fluorescence. Nat Rev Clin Oncol 2013;10:507–18.
[9] Keereweer S, Van Driel PB, Snoeks TJ, Kerrebijn JD, Baatenburg de Jong RJ, Vahrmeijer AL *et al*. Optical image-guided cancer surgery: challenges and limitations. Clin Cancer Res 2013;19:3745–54.
[10] Schaafsma BE, Mieog JS, Hutteman M, van der Vorst JR, Kuppen PJ, Lowik CW *et al*. The clinical use of indocyanine green as a near-infrared fluorescent contrast agent for image-guided oncologic surgery. J Surg Oncol 2011; 104:323–32.
[11] Wang K, Chi C, Hu Z, Liu M, Hui H, Shang W *et al*. Optical molecular imaging frontiers in oncology: the pursuit of accuracy and sensitivity. Engineering 2015;1:309–23.
[12] Zeng C, Shang W, Wang K, Chi C, Jia X, Cheng F *et al*. Intraoperative identification of liver cancer microfoci using a targeted near-infrared fluorescent probe for imaging-guided surgery. Sci Rep 2016;6:21959.
[13] Fang C, Wang K, Zeng C, Chi C, Shang W, Ye J *et al*. Illuminating necrosis: from mechanistic exploration to preclinical application using fluorescence molecular imaging with indocyanine green. Sci Rep 2016;6:21013.

[14] Gabon Q, Sayag D, Texier I, Navarro F, Boisgard R, Virieux-Watrelot D *et al*. Evaluation of intraoperative fluorescence imaging-guided surgery in cancer-bearing dogs: a prospective proof-of-concept phase II study in 9 cases. Transl Res 2016;170:73–88.
[15] He K, Chi C, Kou D, Huang W, Wu J, Wang Y *et al*. Comparison between the indocyanine green fluorescence and blue dye methods for sentinel lymph node biopsy using novel fluorescence image-guided resection equipment in different types of hospitals. Transl Res 2016;178:74–80.
[16] Kim HK, Quan YH, Choi BH, Park JH, Han KN, Choi Y *et al*. Intraoperative pulmonary neoplasm identification using near-infrared fluorescence imaging. Eur J Cardiothorac Surg 2016;49:1497–502.
[17] van Dam GM, Themelis G, Crane LMA, Harlaar NJ, Pleijhuis RG, Kelder W *et al*. Intraoperative tumor-specific fluorescence imaging in ovarian cancer by folate receptor-alpha targeting: first in-human results. Nat Med 2011;17:1315–9.
[18] Liberale G, Vankerckhove S, Caldon MG, Ahmed B, Moreau M, Nakadi IE *et al*. Fluorescence imaging after indocyanine green injection for detection of peritoneal metastases in patients undergoing cytoreductive surgery for peritoneal carcinomatosis from colorectal cancer: a pilot study. Ann Surg 2016; 264:1110–5.
[19] Okusanya OT, DeJesus EM, Jiang JX, Judy RP, Venegas OG, Deshpande CG *et al*. Intraoperative molecular imaging can identify lung adenocarcinomas during pulmonary resection. J Thorac Cardiovasc Surg 2015;150:28–35 e1.
[20] Liu Z, Miller SJ, Joshi BP, Wang TD. In vivo targeting of colonic dysplasia on fluorescence endoscopy with near-infrared octapeptide. Gut 2013;62:395–403.
[21] Lerner SP, Goh A. Novel endoscopic diagnosis for bladder cancer. Cancer 2015;121:169–78.
[22] Okusanya OT, Holt D, Heitjan D, Deshpande C, Venegas O, Jiang J *et al*. Intraoperative near-infrared imaging can identify pulmonary nodules. Ann Thorac Surg 2014;98:1223–30.
[23] Ishizawa T, Masuda K, Urano Y, Kawaguchi Y, Satou S, Kaneko J *et al*. Mechanistic background and clinical applications of indocyanine green fluorescence imaging of hepatocellular carcinoma. Ann Surg Oncol 2014;21:440–8.
[24] Satou S, Ishizawa T, Masuda K, Kaneko J, Aoki T, Sakamoto Y *et al*. Indocyanine green fluorescent imaging for detecting extrahepatic metastasis of hepatocellular carcinoma. J Gastroenterol 2013;48:1136–43.
[25] Tummers QR, Hoogstins CE, Peters AA, de Kroon CD, Trimbos JB, Cj VDV *et al*. The value of intraoperative near-infrared fluorescence imaging based on enhanced permeability and retention of indocyanine green: feasibility and false-positives in ovarian cancer. PLoS One 2014;10:3435–40.
[26] Keating J, Newton A, Venegas O, Nims S, Zeh R, Predina J *et al*. Near-infrared intraoperative molecular imaging can locate metastases to the lung. Ann Thorac Surg 2016;103:390–8.
[27] Yang CFJ, Meyerhoff RR, Mayne NR, Singhapricha T, Toomey CB, Speicher PJ *et al*. Long-term survival following open versus thoracoscopic lobectomy after preoperative chemotherapy for non-small cell lung cancer. Eur J Cardiothorac Surg 2016;49:1615–23.
[28] Venugopal V, Park M, Ashitate Y, Neacsu F, Kettenring F, Frangioni JV *et al*. Design and characterization of an optimized simultaneous color and near-infrared fluorescence rigid endoscopic imaging system. J Biomed Opt 2013;18:126018.
[29] Glatz J, Varga J, Garcia-Allende PB, Koch M, Greten FR, Ntziachristos V. Concurrent video-rate color and near-infrared fluorescence laparoscopy. J Biomed Opt 2013;18:101302.
[30] Onda N, Kimura M, Yoshida T, Shibutani M. Preferential tumor cellular uptake and retention of indocyanine green for in vivo tumor imaging. Int J Cancer 2016;139:673.